J. Bangladesh Acad. Sci. 46(1); 45-55: June 2022 DOI: 10.3329/jbas.v46i1.60346

Journal of Bangladesh Academy of Sciences

Journal homepage: http://www.bas.org.bd/publications/jbas.html

Research Article

Preliminary CFD investigation for secondary coolant in molten salt reactor with alumina nanofluid considering FLiBe and FLiNaK as base fluid through a double pipe heat exchanger

Joy Surjy Deb, Md Mahidul Haque Prodhan*, Nazmul Hossain, and Golam Sarwar Rakib

Department of Nuclear Engineering, University of Dhaka, Dhaka, Bangladesh

ARTICLE INFO

Article History

Received: 22 March 2022
Revised: 29 May 2022
Accepted: 12 June 2022

Keywords: MSR, Nanofluids, Double Pipe Heat Exchanger, CFD, Nuclear Thermal Hydraulics.

ABSTRACT

This work analyzes a computational fluid dynamics (CFD) methodology based on ANSYS to investigate the 3 % and 4 % volume fraction alumina (Al_2O_3) nanofluids with base fluids FLiBe (LiF(67)-BeF_2(33) (mol%)) and FLiNaK (LiF(46.5)-NaF(11.5)-KF(42) (mol%) through a double pipe heat exchanger. The purpose of the paper is to choose better candidates as secondary coolants in molten salt reactors for better thermodynamics performances and heat transfer characteristics. Six secondary coolants with and without nanofluids and fuel salt as primary coolants are driven through the inner and outer pipe. Later overall heat transfer coefficient, outlet temperatures and pressure drops of the fluids, and LMTD are calculated. Thus, this work eventually recommends the best candidate as a secondary coolant by CFD methodology using ANSYS-FLUENT 18.1.

Introduction

The molten salt reactor is one of the advanced generation reactors that may ensure the inherent safety of a nuclear power plant due to its unique safety features like molten salt coolant and fuel. This unique feature provides a distinct advantage over the conventional BWR or PWR fuel rods which might melt over a certain temperature (Cantor et al., 1968). Currently, different researches are being carried on to improve the efficiency of the coolant and enhance the convective heat transfer coefficient and other thermodynamics properties based on their figure of merits. SAMOFAR (Safety Assessment of the Molten Salt Fast Reactor) is a project based on the molten salt fast reactor, one of the leading projects the Europeans manage to ensure the best available molten salt coolant for molten salt nuclear reactors by analyzing their thermal-hydraulic properties with substantial experiments. They have nominated FLiBe and FLiNaK till now (Aniza et al., 2017; Forsberg, 2006; Allibert et al., 2017; Doche et al., 2017; Allibert et al., 2012; Dieuaid, 2018; Marcello et al., 2008). Moreover, nanofluids are showing crucial importance as a coolant in nuclear power plants due to their enhanced material properties and sizes through real-life and simulation-based experiments. Since the last century, many experiments and research have been being contrived, and recently molten salt thermal nuclear power reactors, fast breeder reactors are also initiated in the research arena. Both solid fuels like particles and liquid fuels can be used. As a solid fuel, particles may be incorporated in to a matrix made of graphite. On the other hand, actinides in liquid fuel structure are used, which can be uniformly dispersed in the molten salt directly and kept at very high temperature, coveys inside and outside of the reactor core. In the reactor core, the fuel salt is heated up by the fission reactions of the nuclear elements, and later heat is transferred

*Corresponding author: <prodhan@du.ac.bd>

to the secondary coolant, which subsequently transfers the heat to the tertiary fluid for the power conversion cycle. Most of the previous studies were to investigate the thermal and physical properties of LiF(67)-BeF2(33) (mol%) (FLiBe) and LiF(46.5)-NaF(11.5)-KF(42) (mol%) (FLiNaK) (Aniza et al., 2017; Forsberg, 2006; Williams, 2006; Clarno et al., 2006). Bahri et al. discussed the physical properties of these two molten salts in terms of their application as coolant and fuel solvent and also stated the comparative advantages and disadvantages. Charles et al. analyzed a technology gap to initiate and understand technological challenges for developing and deploying MSRs (molten salt reactors). Williams stated that molten salts seem to be noteworthy candidates because of their strong performances in terms of high temperatures with convenience and flexibility (Williams, 2006; Clarno et al., 2006). Similarly, for the single tube, Hoffman experimentally conducted the forced convective heat transfer performance of FLiNaK salt. (Hoffman and Lones, 1955). Bang et al. (2009) experimented with FLiNaK and gas, where a double pipe heat exchanger was established using small diameter tubes. Primarily, mainly for the SAMOFAR project as a fuel salt which is also a primary coolant, two main options (LiF-ThF4-^{233}UF4) and (LiF-ThF4-^{235}UF4-(Pu-MA)F3) are strongly and significantly recommended (Allibert et al., 2017; Doche et al., 2017). Similarly, Huntly et al. (1976) investigated the forced convective heat transfer of one fuel salt LiF-BeF2-ThF4-UF4 to ensure its competence. While E. Merle investigated another fuel considering the SAMOFAR project (Allibert et al., 2012). Subsequently, CFD based research have been carried on by different academicians to improve heat exchanger as well as to investigate the thermal performances of the fuel and coolant salts, some of which are also considered to use in the SAMOFAR project as well as for future purposes; some CFD based modeling methods have been proposed too (Rubiolo et al. 2017). Cammi et al. (2019) investigated and referred to two promising technologies and also presented preliminary results on the Printed Circuit and the Helical Coil heat exchangers to improve heat transfer efficiency. Dieuaid (2018) has analyzed neutronic and thermal analyses like decay heat and re-criticality of molten salt reactors considering the SAMOFAR project using MCNPX to introduce reprocessing unit design. In addition, Marcello et al. conducted research with the help of COMSOL Multiphysics® to investigate and determine the coupled dynamics considering both nuclear and thermal parts (Marcello et al., 2008). Kasam and Shwageraus (2017) conducted CFD simulations for a single fuel tube which were performed with varying parameters to establish the relationship between the maximum fuel temperature and parameters such as fuel salt properties, tube diameter, and power density. Moreover, several CFD types of research were conducted to determine the thermal- hydraulics performances of the coolant in designed shell and tube heat exchangers and improve the heat exchangers for better heat transfer conditions (Fraas and Laverne, 1971; Bettis et al., 1967). Köse et al. (2019) investigated and proposed a heat exchanger design for SAMOFAR using ANSYS FLUENT commercial code. Chi et al. (2011) examined the thermal-hydraulic characteristics such as the Nusselt number of the molten salt LiF(46.5)-NaF(11.5)-KF(42) using Gnielinski and Hausen correlations that are considered more appropriate than Dittus- Boeltar in terms of molten salt (Gnielinski, 1976; Hausen, 1959). However, Ambrosek et al. recently re-evaluated the FLiNaK test data with an updated formula which eventually showed an improved relation according to the Dittus-Boelter correlation with a minor 15 percent error (Ambrosek et al., 2009). Apurba used Hausen and Gnielinski correlations for evaluating molten nitrate heat transfer (Anderson et al., 2015). Nanofluids are also contributing a significant part to the future nuclear industry and its research arena for safe operation and ensuring enhanced heat transfer rate. Choi et al. (2001) investigated nanofluids of different elements and observed a 40% increase that is significant in terms of thermal conductivity for Cu-containing ethylene glycol. Li and Xuan (2003)

examined the convective heat exchange and the stream highlights of Cu-water nanofluids at a -10 mm inward distance across the tube, which eventually provided a positive output. Rea (Buongiorno et al., 2012) led an investigation on the laminar convective warmth exchange and weight drop of alumina– water and zirconia-water nanofluids in a tube with a 4.5 mm inward width. Their discoveries illustrated that there is no deviation in convective heat exchange and weight drop of nanofluid spill out of customary single-stage stream hypothesis with appropriately measured nanofluid properties. Etemad et al. (2006) played out an exploratory investigation to decide that alumina nanoparticles are more beneficial than CuO nanoparticles in terms of the same volume and Reynolds number. Ding and Wen (2004) examined alumina nanoparticles and de-ionized water for heat transfer calculation and eventually concluded that heat transfer increases using nanofluid. Allahyari et al. (2011) studied laminar mixed convection of alumina water by heating the top half surface of a Cu tube horizontally. They concluded that the heat transfer coefficient rises with the increased concentration of nanoparticles. Sarma experimented with water-based alumina nanofluids and calculated the increase of convective heat transfer for different Reynolds numbers with constant wall heat flux (Sarma et al., 2009). Buongiorno proposed a mathematical model by considering nanoparticle/base fluid slip, and he showed that Brownian motion and thermophoresis are the main mechanisms for this slip mechanism (Buongiorno, 2006). On the other hand, Kleinstreuer and Koo (2004) proved that Brownian motion was the more important phenomenon. Also, the thermal conductivity of nanofluids has strong temperature dependence. Evans et al., (2006) proved that the direct influence of the Brownian motion of the nanoparticles via diffusion is negligible. Aybar et al. (2009) did experimental investigations that support the indirect influence of the Brownian motion regarding nanofluids' higher heat transfer characteristics. Choi and Jang (2007) proposed a model based on Brownian motion-induced nano-convection. The model proposed by Kumar et al. (2004) based on Brownian motion overestimated the contribution of Brownian motion to heat flow. But Das et al. (2005) improved the model proposed by Kumar et al. by incorporating the effect of micro convection due to particle movement. Trivedi (2008) found that decreasing the temperature of a component increases its performance, such as reliability. Das and Vajjha (2009) presented the dependency of thermal conductivity on both temperature and nanoparticle concentration. Hadad et al. (2013) investigated the thermal-hydraulic properties of $Al_2O_3^+$ water nanofluid as the coolant in a VVER-1000 nuclear reactor core by using a CFD code considering a finite volume method for single-phase and two-phase mixture models to find convective heat transfer coefficient and pressure drop. Similarly, in a study done by Boungiorno et al. (2017), nanofluids are used as the main reactor coolant for pressurized water reactors (PWRs), which could be used to enhance economic performance with at least 32% higher critical heat flux (CHF) and a 20% power density commensurate with current PWRs without varying the fuel assembly design and without decreasing the margin to CHF. However, to date, not many experiments have been conducted with a mixture of nanofluids with FLiBe or FLiNaK as a nuclear coolant. Therefore, this paper will analyze this promising aspect of nanofluids in molten salt reactors, considering the fuel salt and secondary coolant salt for the SAMOFAR project.

Mathematical Model Governing Equations

Before the simulation, this work assumed some significant criteria. Firstly the rate of turbulence energy ε. These two parameters k and ε can be found by solving the following equations (Choi and Jang, 2017; Aybar et al., 2009). The simulation was conducted under steady-state conditions. The vital governing equations that were used to simulate the thermal-hydraulic characteristics include the continuity, momentum, and energy equations (Li and Xuan, 2003; Li et al., 2019). Besides, the appropriate

turbulence model was integrated to conduct the simulation. For steady-state conditions. The following equation (Li et al., 2019) can be described as below:

Continuity Equation

$$\nabla.(\rho u) = 0 \quad \text{..... (3.1)}$$

Momentum Equation

$$\nabla.(\rho u u) = -\nabla.p + \nabla.\tau \quad \text{..... (3.2)}$$

τ is the stress tensor (described below),

$$\tau = \mu\,[(2\nabla.u) - \tfrac{2}{3}\nabla.u] \quad \text{..... (3.3)}$$

Energy Equation

$$\nabla \cdot (\rho u h) = \nabla \cdot \left(\left(\frac{\Gamma}{C_p}\right)\nabla.u\right) \quad \text{..... (3.4)}$$

Turbulence Model

Since the Reynolds number is greater than 2300 in pipe flow, the influence of turbulence must be considered. In the present work, a standard k-ε turbulence model is employed. The standard k-ε model includes two transport equations: turbulence kinetic energy k and dissipation rate of turbulence energy ε. These two parameters, k and ε, can be found by solving the following equations (Choi and Jang, 2007; Aybar et al., 2009).

$$\frac{\partial}{\partial x_i}(\rho k u_i) = \frac{\sigma}{\partial x_j}\left[(\mu + \mu_t/\sigma_k)\frac{\sigma\kappa}{\partial x_j}\right] + G_k - \rho\epsilon \quad \text{..(3.5)}$$

$$\frac{\partial}{\partial x_i}(\rho\epsilon u_i) = \frac{\partial}{\partial x_j}\left[(\mu + \mu_t/\sigma_\epsilon)\frac{\partial}{\partial x_j}\right] + C\epsilon_1(\epsilon/k)\,G_k - C\epsilon_2(\epsilon^2/k)\,\rho \quad \text{.....(3.6)}$$

Here, turbulence viscosity, $\mu_t = \rho\, C\mu\, (k^2/\epsilon)$ G_k is the production of turbulent kinetic energy and $G_k = \rho\overline{u'_i u'_j}\frac{\partial u_j}{\partial x_i}$, $C\epsilon_1$, $C\epsilon_2$, $C\mu$, σ_k ∂x_i and σ_ϵ are empirical constants where, $C\epsilon_1 = 1.44$, $C\epsilon_2 = 1.92$, $C_\mu = 0.9$, $\sigma_k = 1$ and $\sigma_\epsilon = 1.3$

Simulation

Geometry and Boundary Condition

This work investigates a preliminary concept of a double pipe heat exchanger. Though a double pipe heat exchanger is not considered significant in real life, it demonstrates a brief analysis of the effect of alumina nanofluids with FLiBe and FLiNaK as secondary coolants regarding the overall heat transfer coefficient, cycle efficiency, and pressure drop of the coolants. For meshing multi-zoned meshing method with Hexa mapped mesh type is used. In the meshing section also, inflation is controlled to ensure first layer thickness competence and increase meshing quality. As the standard k epsilon method is introduced, the wall Y+ value is adjusted between the value of 30-100, and thus the meshing is employed bearing that for the simulation. The SIMPLE method is employed to couple velocity and pressure here. According to different previous works, nanofluids can be treated as single-phase models for low volume fractions (Singh and Sundar, 2013; Mujumdar and Wang, 2008). As the volume fraction of 3% and 4% are considered for this work, the single-phase method is employed here. In this investigation, computational fluid dynamics (CFD) code FLUENT 18.1 is used as an analysis tool; it utilizes the continuity equation, momentum equation, energy equation, and standard K- epsilon turbulence model. A double pipe heat exchanger has been introduced to determine the better secondary coolant out of the proposed candidates above. For this simulation, t = 5 mm; D_i = 50 mm; D_o = 45 mm; L_i = 1.3 m; L_o = 1 m.

To conduct this experiment, as a fuel salt ^{7}LiF(77.5)-ThF4(20)-^{233}UF3(2.5) (%mol) is selected, which is forced to travel through the inner pipe. The inlet velocity for the fuel salt is 2.5 ms^{-1}. Similarly, for the six secondary coolant candidates, which are also forced to pass through the outer pipe, the inlet velocity is selected 5 ms^{-1}. The Inlet temperature for the inner pipe is 1023K, while for the outer pipe, it is 833K. In addition, the pressure is kept at 1-2 atm. These data are selected based on several studies and recommended operating temperature, pressure, velocity, and other operating conditions (Cammi et al., 2019; Köse et al. 2019).

Thermal Properties

For Pipe material, it has been suggested to use hastelloy-n alloy for its higher melting point, and better strength and physical since MSRs need to

operate at a higher temperature compared to conventional PWR and BWR power plants (Williams, 2006; Carno et al. 2006; Hoffman and Lones, 1955). The thermal properties of the fuel salt, secondary coolant candidates, and hastelloy-n alloy are selected by different empirical equations and data from several studies. Allibert et al. (2012) represented empirical equations to determine the thermal and physical properties of the fuel salt, which is calculated for a temperature of 1023K for this experiment. Moreover, for hastelloy-n alloy, this data is selected from another study (Kedl, 1970). In addition, the thermal and physical data of FLiBe and FLiNaK have been derived from another study for 973K (Ebner et al., 2010). According to work mentioned above, the thermal properties of FLiBe, FLiNaK, and Hastelloy-n alloy are given in Table-1 for 700°C, whereas; for alumina nanofluids, the data is considered at 25°C (Chukwu et al., 2006).

Table 1. Thermal properties of the coolant and materials

Name	Specific Heat ($JKg^{-1}K^{-1}$)	Thermal Conductivity ($Wm^{-1}K^{-1}$)	Density (kgm^{-3})	Viscosity (Pa.s)
FLiBe	2397.73	1.1163	1938.06	0.0055
FLiNaK	2011.7	0.9050	2018.9	0.0025
Hastelloy-n	578	23.6	8860	
Alumina	773	36	3880	

Similarly, for 3% and 4% alumina nanofluid with base fluid molten salt coolant (FLiBe and FLiNaK), all the thermophysical properties are derived from the following equations (Chukwu et al., 2006), where ø is the volume percentage of the nanoparticles in the base fluid, whereas; nf and bf mean nanofluid and base fluid respectively.

$$\rho_{nf} = (1-ø)\,\rho_{nf} + ø \times \rho_p \quad (4.1)$$

$$(\rho C_p)_{nf} = (1-ø)\,(\rho C_p)_{bf} + ø \times (\rho C_p)_p \quad (4.2)$$

$$\mu_{nf} = (123ø^2 + 7.3ø + 1)\mu_{bf} \quad (4.3)$$

$$k_{nf} = (4.97ø^2 + 2.72ø + 1)k_{bf} \quad (4.4)$$

Results and Discussions

The fuel salt and the six candidates are forced to be conveyed through the double pipe heat exchanger. The average overall heat transfer coefficient is found along with LMTD and pressure drop in both pipes and the outlet temperature of both fluids (inner and outer). For analyzing this data, some equations related to thermodynamics are used.

$$Qi = \dot{m}\, cph\, (t_{hi} - t_{ho}) \quad (5.1)$$

$$Qo = \dot{m}\, cpc\, (t_{co} - t_{ci}) \quad (5.2)$$

$$LMTD = (\Delta T_1/\Delta T_2)/[\ln(\Delta T_1/\Delta T_2)] \quad (5.3)$$

$$Q_{avg} = Q_i + Q_o \quad (5.4)$$

$$U = Q_{avg} / (A_s \times LMTD) \quad (5.5)$$

Where, $\Delta T_1 = t_{hi} - t_{co}$; $\Delta T_2 = th_o - t_{ci}$,
and $A_s = \pi D_o L_o$

From Fig.1 and Table 2, it can be derived that with increasing nanofluid volume percentage in base molten salt for both FLiBe and FLiNaK as secondary coolant, the pressure drop in terms of

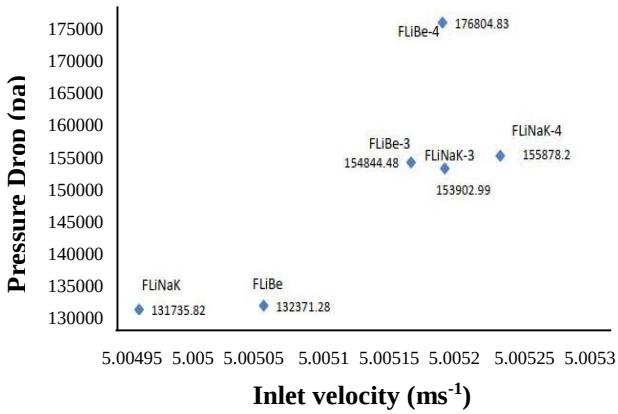

Fig. 1. Outer pipe inlet velocity vs. pressure drop for secondary coolant candidates.

Table 2. Outer Fluid' Reynolds Number and Mean Velocity

Name	Reynolds Number	Mean Velocity (ms^{-1})
FLiBe	792842.73	5.00253155
FLiBe-3	615303.55	5.00258795
FLiBe-4	553098.7317	5.0026
FLiNaK	1817010	5.00248385
FLiNaK-3	1414590.682	5.0026009
FLiNaK-4	12722979.459	5.0026221

secondary coolant has been increased, indicating that a higher power required to pump in case of a real application with nanofluids than an conventional plan without nanofluids. The explanation behind that is quite convenient and simple. According to available friction factor correlations, the friction factor will increase smooth pipe for turbulent and higher Reynolds number flow, with higher viscosity and lower Reynolds number of the fluid for the same inlet velocity. Thus the pressure drop will increase too (Srichai S). From the table, it can be seen that for both base fluids with a higher percentage of nanofluids, the Reynolds number decreases for the same inlet velocity 5 ms^{-1}. In contrast, the viscosity is increasing according to equation no. 4.3 that has been previously discussed. Physically, in turbulent flow, fluid mixing at different layers is very significant and high. Therefore, the average velocity gradient doesn't vary significantly in these regions. However, this cannot happen near the wall since the fluid follows no-slip condition. So, a large change in velocity has to occur within a very thin region (laminar sub-layer), resulting in a very high gradient. Moreover, in a given regime, the friction factor decreases with increasing Reynolds number since when Re increases, the gradient (du/dy) also increases but at a lesser rate. Moreover, with higher viscosity of the fluids means higher probabilities of collisions between fluid layers that eventually increase pressure drop. In Fig. 2, the contour image of the pressure distribution of the six secondary coolants has been shown has been developed after simulation.

From Fig. 3, it can be shown that with increasing nanofluid volume percentage in FLiBe, the outlet temperature of the fuel salt is decreased, indicating transferring a higher amount of energy to the secondary coolant. Nevertheless, in the case of FLiNaK, it demonstrates, unlike FLiBe. With

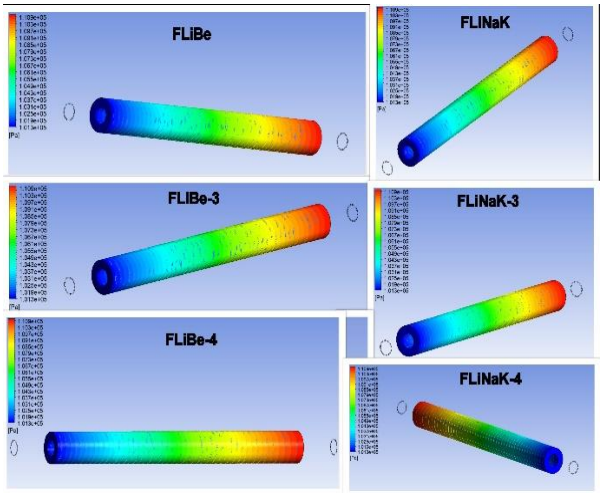

Fig. 2. Contour image of the secondary coolants' pressure distribution

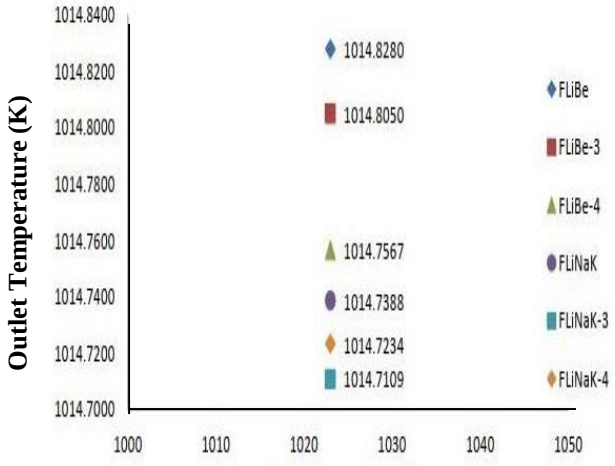

Fig. 3. Fuel salt's inlet temperature vs. outlet temperature for different secondary coolants.

FLiNaK as a secondary coolant, the fuel salt has the highest outlet temperature like FLiBe in the previous case. However, the lowest value of outlet temperature of fuel salt is in the case for FLiNaK-3 as a secondary coolant instead of FLiNaK-4 with a difference of 0.0125 K, which is a convoluted case and mysterious.

In Fig. 4, the contour image of the temperature distribution of the fuel salts in terms of the six different secondary coolants has been shown that has been developed after simulation.

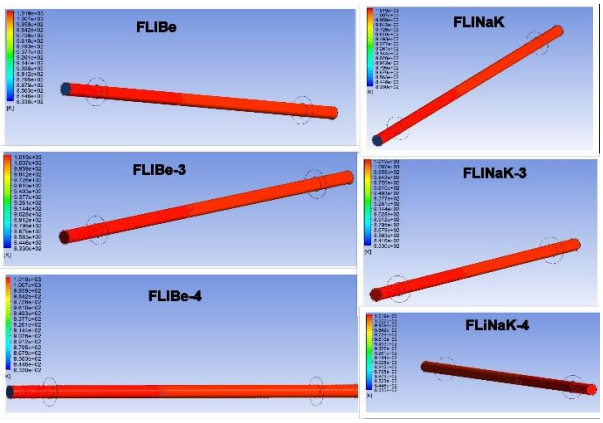

Fig. 4. Contour image of fuel salt's temperature in case of different secondary coolants.

Nonetheless, in Fig. 5, the results are as expected. In both FLiBe and FLiNaK cases, with the gradually increasing nanofluids volume percentage, the outlet temperature has also increased conveniently, and FLiBe-4 and FLiNaK-4 have come out best secondary coolants compared with their base fluids. In the following Fig. 6, the contour image of the six secondary coolants' temperature distribution has been developed after simulation.

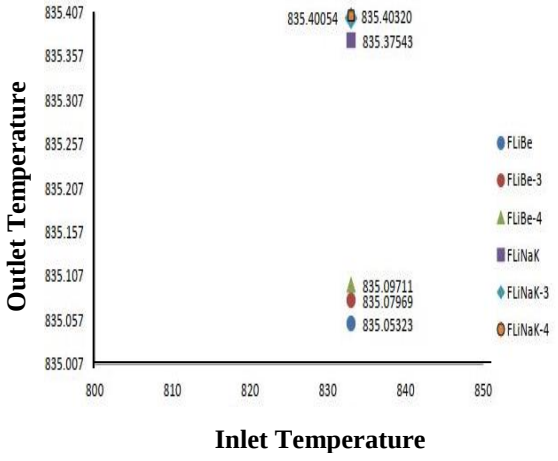

Fig. 5. Outer pipe inlet temperature vs. outlet temperature for secondary coolant candidates.

Fig. 7, illustrates that with the overall heat transfer coefficient increased with increasing Nano fluid volume percentage. At the same time, LMTD showed a decreasing trend in the case for FLiBe, whereas for the FLiNaK case, FLiNaK have been

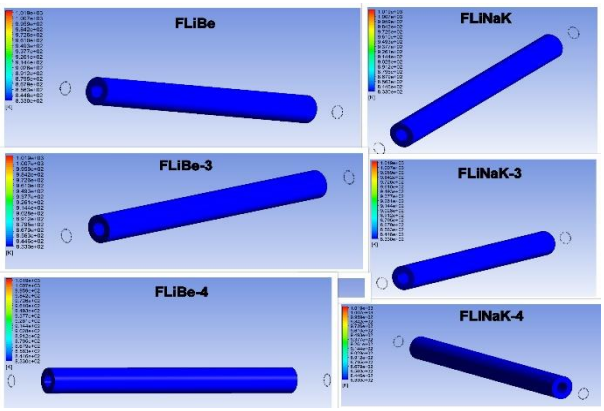

Fig. 6. Contour image of secondary coolants' temperature distribution.

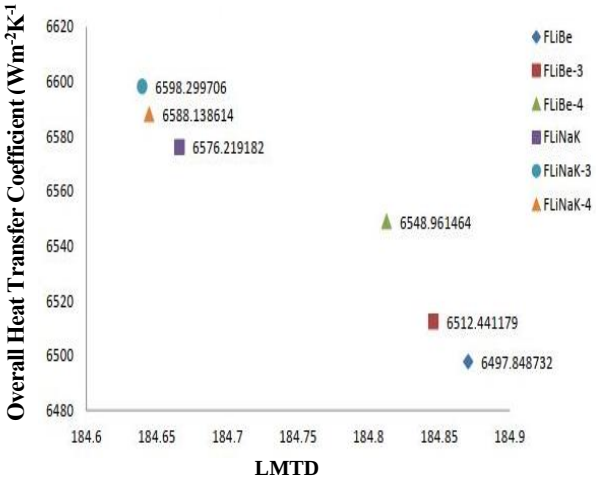

Fig. 7. LMTD vs. overall heat transfer coefficient for double pipe heat exchangers.

shown the lowest overall heat transfer coefficient and highest LMTD. However, the highest overall heat transfer coefficient and lowest LMTD have been found whenever FLiNaK-3 is used instead of FLiNaK-4 as a secondary coolant for the same fuel salt.

To summarize, it can be stated that by increasing nanofluid volume percentage gradually, the overall heat transfer coefficientand the outlet temperature of the secondary coolant have been increased for FLiBe. This indicates a positive output of the study.

Therefore, the heat exchanger area can be reduced whenever nanofluid is used, securing an economic

benefit. Because less area means less material is to be used for heat exchangers, which are expensive enough to withstand the high temperature.

The reason behind the nanofluids' positive impact can be explained by analyzing thepositive impact of nonofluids' Brownian motion and the higher wettability of the nanofluids compared to base fluids. The Brownian motion in nanofluids is significant compared to base fluids due to their nano-scale molecular presence, it transfers heat more conveniently than the base fluids. Moreover, due to its higher surface to volume ratio, it can easily create and continue contact between the solid surface of the pipe more conveniently and efficiently than the base fluid, thus increasing the heat transfer compared with the latter one. In addition, since the outlet temperature of the secondary coolant is increased, it will help enhance the efficiency of the power conversion loop later. But one distinct disadvantage of this experiment is that whenever there is an increased amount of nanofluid in FLiBe, the pressure drop pump's shows an increasing trend, which determines the power an economic setback.

For FLiNaK, it is clear that coolant with nanofluid is better than without using it in the first place, and it almost showed positive results like FLiBe. Nevertheless, there is a convoluted output. Instead of FLiNaK-4, FLiNaK-3 showed the best overall heat transfer coefficient, while FLiNaK-4 showed the best outlet temperature for coolant. The result is not as expected. The probable explanation for this matter can be about the heat exchanger dimension and less contact area to find positive feedback properly. It might also be solved with the finest meshingtechniques. Nonetheless, it is known that the temperature drop in fuel salt shouldn't exceed 100 K and for coolant, it should be around 50 K. Bearing that in mind, FLiNaK-4 may be a better candidate. However, the results difference was not significant enough. It can be overlooked due to the double pipe heat exchanger system. These results will be more significant with a more refined and rigorous shell and tube heat exchanger design.

Conclusions

Nanofluid plays a key role in enhancing heat transfer quality for nuclear reactors. This study illuminates the idea of using nanofluid in MSRs. This study has found out that, in the case of FLiBe, the outcome is satisfactory for using nanofluid and can be vouched for using it. However, in the case of FLiNaK, the study produced a convoluted outcome. Despite ensuring nanofluids superiority, the best option between FLiNaK-3 and FLiNaK-4 cannot be chosen without a doubt. In the future, with shell and tube heat changers, this proposal can be verified more providently and rigorously. Moreover, the neutronic analysis should also be conducted to ensure its criticality and maintain the safety and positive output of the reactors. Similarly, an opportunity cost may be decided between expensive heat exchanger material and a higher power pump, obviously with a detailed analysis of the findings.

Conflicts of Interest

The authors declare that they have no conflicts of interest regarding the publication of this article

Author's Contributions

Joy Surjy Deb: Concepts, Literature review, Simulation, analysis, Formatting, manuscript writing and revision.

Md. Mahidul Haque Prodhan: Concepts, Literature review, simulation, supervision, manuscript writing, analysis correction, and revision.

Nazmul Hossain: Literature review, result analysis, Formatting, and manuscript writing.

Golam Sarwar Rakib: Literature review, Formatting, and manuscript writing.

Nomenclature

u = fluid velocity

ρ = fluid density

η = stress tensor

Γ = fluid thermal conductivity

k = turbulence kinetic energy

ε = turbulence dissipation rate

μ_t = turbulence viscosity

G_k = production of turbulence kinetic energy

t = inner pipe thickness
D_i = inner pipe diameter
D_o = outer pipe diameter
L_i = inner pipe length
L_o = outer pipe length
t_{ci} = inlet temperature of fuel salt
t_{co} = outlet temperature of fuel salt
Q_i = amount of heat transfer taking place in fuel salt
Q_o = amount of heat transfer taking place in coolant salt
LMTD = logarithmic mean temperature difference
U = overall heat transfer coefficient
A_s = outer surface area of the inner pipe
k = thermal conductivity of hastelloy-nalloy

References

Allahyari S, Behzadmehr A and Sarvari SMH. Conjugate heat transfer of laminar mixed convection of a nanofluid through a horizontal tube with circumferentially non-uniform heating. *Nanoscale Res. Lett.* 2011; 6: 360.

Allibert M, Merle-Lucotte E, Heuer D, Brovchenko M and Ghetta V. Preliminary design assessment of the molten salt fast reactor. European Nuclear Conference (ENC 2012), Dec 2012, Manchester, United Kingdom. pp. 17-26. (in2p3-00766659).

Ambrosek J, Allen T, Anderson M, and Sridharan K. Current status of knowledge of the fluoride salt (FLiNaK) heat transfer. *Nucl. Tec.,* 2009; 165(2): 166-173.

Anderson MH, Clark MM, Das AK, Fiveland WA and Teigen BC. Heat transfer behavior of molten nitrate salt. In AIP Conference Proceedings, Solar, PACES. 2015; 1734(1): 040003. 1-8.

Aniza CN, Bahri CB, Al Areqi WM, Majid AAB and Ruf MIFM. Characteristic of molten fluoride salt system LiF-BeF2 (Flibe) and LiF-NaF-KF (Flinak) as coolant and fuel carrier in molten salt reactor. In: *AIP Conference Proceedings*, 2017; 1799(1): 040008.1-8.

Aybar HS, Azizian MR and Okutucu T. Effect of nanoconvection due to Brownian motion on thermal conductivity of nanofluids. In: *Proceeding of the 7th IASME/WSEAS International Conference on Heat Transfer, Thermal Engineering and Environment*, Moscow 2009; pp. 53-55

Bang KH, Choi OK, Hwang, IS, Jeong HS, and Kim KK. An experimental study on the flow and heat transfer of flinak molten salt in small channels for the application to the VHTR intermediate heat exchanger. In: *Proceedings of international congress on advances in nuclear power plants*, 2009, p. 2572.

Bettis CE, Braatz RJ, Cristy GA, Dyslin DA, Kelly OA, Pickel TW, Shobe LR, Spaller AE and Stoddart WC. Design study of a heat-exchange system for one MSBR (Molten Salt Breeder Reactor) concept, Oak Ridge National Laboratory, Tennessee, USA, 1967; Tech. Rep.TM-1545.

Boungiorno J, Forrest E, Hannink R, LW, Kim SJ and Truong B. Nanofluids for enhanced economics and safety of nuclear reactors: an evaluation of the potential features, issues, and research gaps. *Nucl. Tec.*, 2017; 162: 80-91.

Buongiorno J, Hu LW, McKrell T and Rea U. Laminar convective heat transfer and viscous pressure loss of alumina- water and zirconia-water nanofluids. *Int. J. Heat Mass Transf.* 2012; 52, 2042-2048.

Buongiorno J. Convective transport in nanofluids. *J. Heat Transf.* 2006; 128(3): 240-250.

Cammi A, Lorenzi S and Ronco A. Preliminary analysis and design of the heat exchangers for the molten salt fast reactor. *Nucl. Eng. Tec.*, 2019; 52(1): 51-58.

Cantor S, Cooke JW, Dworkin AS, Robbins GD, Thomas RE and Watson GM. Physical properties of molten-salt reactor fuel, coolant, and flush salts. Oak Ridge National Laboratory, Tennessee, USA, 1968; Tech. Rep. TM-2316.

Chi CW, Ferng YM and Kun-Yueh Lin. CFD investigating thermal-hydraulic characteristics of FLiNaK salt as a heat exchange fluid. *App. Ther. Eng., 20*12. 37: 235-240.

Choi SUS and Jang SP. Effects of various parameters on nanofluid thermal conductivity. *J. Heat Transf.* 2007; 129(5): 617-623.

Choi SUS, Eastman JA, Li S, Thompson LJ and Yu W. Anomalously increase effective thermal conductivities of ethylene glycol-based nanofluids containing copper nanoparticles. *Appl. Phy. Lett.*, 2001; 78 (6): 718-720.

Chukwu GA, Das DK and Kulkarni DP. Temperature dependent rheological property of copper oxide nanoparticles suspension (nanofluid). J. Nanosci. Nanotechnol., 2006; (4): 1150-1154.

Clarno KT, Toth LM and Williams DF. Assessment of candidate molten salt coolants for the advanced high- temperature reactor (AHTR). Oak Ridge National Laboratory, Tennessee, USA, 2006; Tech. Rep.TM-2006/12.

Das DK and Vajjha RS. Experimental determination of thermal conductivity of three nanofluids and development of new correlations. *Int. J. Heat Mass Transf.* 2009; 52(21-22): pp. 4675-4682.

Das SK, Dasgupta A, Dasgupta N, Patel HE, Sundararajan T and Pradeep T. A micro-convection model for thermal conductivity of nanofluids. *Pramana J. Phys*. 2005, 65: 863-869.

Dieuaide M. SAMOFAR molten salt fast reactor reprocessing unit design.

Ding Y and When DS. Experimental investigation into convective heat transfer of nanofluids at the entrance region under laminar flow conditions. *Int. J. Heat Mass Transf.* 2004; 47(24): 5181-5188.

Doche O, Rubiolol P and Tano M. Progress in modeling solidification in molten salt coolants. *Mod. Sim. Mat. Sci. Eng.*, 2017; 25: 074001.

Ebner MA, Sabharwall P, Sharpe P and Sohal MS. Engineering database of liquid salt thermophysical and thermochemical properties, Idaho National Laboratory, Idaho, USA, 2010; Tech. Rep. INL/EXT-10-18297.

Etemad SG, Esfahany MN and Heris SZ. Experimental investigation of oxide nanofluids laminar flow convective heat transfer. *Int. Com. Heat Mass Transf.* 2006; 33(4): 529-535.

Evans W, Fish J and Keblinski P. Role of Brownian motion hydrodynamics on nanofluid thermal conductivity. *Appl. Phy. Let.*, 2006; 88(9): 093116.

Forsberg CW. Molten-salt-reactor technlogy gapsk. In: Proceedings of ICAPP, USA, 2006; Article ID 6295: pp. 1-8.

Fraas AP and Laverne ME. Parametric survey of the effects of major parameters on the design of fuel-to-inert-salt heat mchangees for the msbr. Oak Ridge National Laboratory, Tennessee, USA, 1971; Tech. Rep. TM-2952.

Gerardin D, Allibert M, International Conference on Fast Reactors and Related Fuel Cycles: Next Generation Nuclear Systems for Sustainable Development. Yekaterinburg, Russia 2017; p. 129.

Gnielinski V. New equations for heat and mass transfer in turbulent pipe and channel flow. *Int. Chem. Eng.*, 1976; 16 (2): 359-367.

Hadad K, Rahimian A and Nematollahi M. Numerical study of single and two- phase models of water/Al2O3 nanofluid turbulent forced convection flow in VVER-1000 nuclear reactor. *Ann. Nucl. Energy*, 2013; 60: 287-294.

Hausen H. Neue gleichungen für die wärmeübertragung bei freier oder erzwungener stromüng (new equations for heat transfer in free or forced flow). *Allg. Wärmetechn*; 1959; 9: 75-79.

Hoffman HW and Lones J. Fused salt heat transfer, part II: forced convection heat transfer in circular tubes containing NaF-KF-LiF eutectic. Oak Ridge National Laboratory, Tennessee, USA, 1955; Tech. Rep.1777; Corpus ID: 137946943.

Huntley WR, Robertson HE and Silverman MD. *Heat transfer measurements in a forced convection loop with two molten-fluoride salts: LiF–BeF2-ThF4–UF4* and *EUTECTIC NaBF4–NaF*. Oak Ridge National Laboratory, Tennessee, USA, 1976; Tech. Rep. TM- 5335.

Kasam A and Shwageraus E. Approximate heat transfer solution for the breed and burn molten salt reactor. In: International Conference on Mathematics & Computational Methods Applied to Nuclear Science & Engineering, Korea, 2017; P146S02-07.

Kedl RJ. Fluid dynamic studies of the molten-salt reactor experiment (msre) core, Oak Ridge National Laboratory, Tennessee, USA, 1970; Tech. Rep. TM- 3229.

Kleinstreuer C and Koo J. A new thermal conductivity model fornanofluids. J. Nanoparticle. Res., 2004; 6(6): 577-588.

Köse U , Koç U, Erbay LB , Öğüt E and Ayhan H. Heat exchanger design studies for molten salt fast reactor. EPJ Nuclear Sci. Technol., 2019; 5: 12.

Kumar DH, Patel HE, Kumar VRR, Sundararajan T, Pradeep T and Das SK. Model for heat conduction in nanofluids. *Phy. Rev. Lett.* 2004; 93(14): 144301.

Li M, Ning B, Qiu Y and Zhang H. Numerical and experimental study on heat transfer and flow features of representative molten salts for energy applications in turbulent tube flow. *Int. J. Heat Mass Transf.* 2019; 135: 732-74.

Li Q and Xuan Y. Investigation on convective heat transfer and flow features of nanofluids. *J. Heat Transf.* 2003; 125(1): 151-155.

Marcello V, Cammi A and Luzzi L. Analysis of coupled dynamics of molten salt reactors. In: *Proceedings of the COMSOL Conference*, Hannover, Germany, Poster Presentation, 2008.

Mujumdar AS and Wang X. A Review on Nanofluids - part I: Theoretical and Numerical Investigations. *B. J. Chem. Engr.*, 2008; 25(4): 613-630.

Rubiolo PR, Retamales MT, Ghetta VE and Giraud J. High temperature thermal hydraulics modeling of a molten salt: application to a molten salt fast reactor (MSFR). In: *ESAIM: Proc. Surv.*, 2017; 58: 98-117.

Sarma PK, Sharma KV and Sundar LS. Estimation of heat transfer coefficient and friction factor in the transition flow with low volume concentration of Al_2O_3 nanofluid flowing in a circular tube and with twisted tape insert. *Int. Com. Heat Mass Transf.* 2009; 36(5): 503-507.

Singh MK and Sundar LS. Convective heat transfer and friction factor correlations of nanofluid in a tube and with inserts: A review. *Renew. Sustain. Energy Rev.*, 2013; 20: 23-35.

Srichai S. Friction factors for single phase flow in smooth and rough tubes, Thermopedia. doi: 10.1615/ A to Z.f.friction_factors_for_single_phase_flow_in_smooth _and_rough_tubes.

Trivedi A. Thermo-mechanical solutions in electronic packaging: component to system level. M.Sc. dissertation, Dept. Mechanical. Eng., The University of Texas, Arlington, Texas, USA, 2008.

Williams DF. Assessment of candidate molten salt coolants for the ngnp/hi heat transfer loop. Oak Ridge National Laboratory, Tennessee, USA, 2006; Tech. Rep. TM-2006/69.